

Transport of Reacting Solute in a One-Dimensional, Chemically Heterogeneous Porous Medium

WILLEM JAN P. BOSMA AND SJOERD E. A. T. M. VAN DER ZEE

Department of Soil Science and Plant Nutrition, Agricultural University, Wageningen, Netherlands

Reacting, nonlinearly adsorbing solute transport in chemically heterogeneous soils is studied. Assuming adsorption is adequately described with the Freundlich equation, random variation of the adsorption coefficient is assumed to describe the heterogeneity. In a homogeneous case, traveling wave fronts develop, characterized by a constant velocity and a constant front shape. Using the method of moments, an analytical expression is derived to describe the constant variance of the traveling wave front. Deviations from the analytical variance and velocity, both calculated with an average adsorption coefficient, show that column scale heterogeneity has significant effects on front spreading and front movement. Expected values of front velocity and variance are computed as averages of values of 600 randomly generated columns. The nonlinear process causes small deviations from the case with average parameters. The ensemble average concentration front, representing an average front for the flow domain, shows that three mechanisms are responsible for the front spreading. At early displacement times the front spreading is caused by the thickness of the individual traveling waves. Subsequently, the effect of the internal variation of the adsorption coefficient (column scale heterogeneity) increases, whereas at large displacement times the front spreading is dominated by the different retardation coefficients of the different columns. The latter effect causes the variance to increase in proportion to t^2 . An analytical approximation is derived for the ensemble average front, ignoring column scale heterogeneity.

INTRODUCTION

The contamination of the environment has become a matter of considerable concern. In areas with high intensity of industry and agriculture, large concentrations of heavy metals or organic contaminants may reach the soil by atmospheric deposition or by waste disposal. These contaminated sites are a potential risk for groundwater quality, for the quality of agricultural production, and for the quality of the drinking water supply. In order to manage our soil and groundwater resources properly, modeling tools are necessary to understand and predict movement of contaminants in the environment.

During the past decades much attention has been given to the theory and modeling of solute transport. This development has been accelerated and increased by the difficulty and high costs of field scale measurements. Much attention has been given to one-dimensional monocomponent solute transport in homogeneous media. Monocomponent models may adequately describe situations where nonreacting solutes or solutes at trace levels are present [van der Zee, 1990b]. A number of analytical solutions for these cases, for different boundary conditions, were given by van Genuchten and Alves [1982], who considered linear adsorption and zeroth- and first-order production and decay. Extensions were developed, taking into account the nonequilibrium aspect of the adsorption process, by van Genuchten *et al.* [1974] and Rao *et al.* [1979].

Many transport models concern homogeneous media, but in practice soils and groundwater systems appear to be heterogeneous. One of the first efforts to describe heterogeneity was achieved by making use of the dual-porosity concept [Coats and Smith, 1964; van Genuchten and Wierenga, 1976] and of the two-site surface adsorption

concept [Cameron and Klute, 1977]. In some cases heterogeneity may be treated deterministically (e.g., in the case of well-defined layers with different texture or composition that are separated by relatively sharp interfaces). Valocchi [1989] studied the effect of a stratified aquifer on (two-dimensional) longitudinal solute spreading. He found that pore scale dispersion, column scale heterogeneity and adsorption kinetics are three dominating front-spreading factors. However, in order to study heterogeneity in general cases a stochastic approach may be necessary. One of the first stochastic approaches for nonreactive solute transport was given by Dagan and Bresler [1979] and Bresler and Dagan [1979, 1981, 1983]. By linearizing the flow equation Dagan [1988, 1989] derived an analytical solution for the spreading process of a nonreactive solute, taking into account a lognormal distribution of the hydraulic conductivity. It was shown that for a nonreactive solute, spatial variability of hydraulic conductivity accounts for a much larger solute spreading than pore scale dispersion. Bellin *et al.* [1992] validated Dagan's linear solution with extensive numerical calculations. Graham and McLaughlin [1991] applied a technique which uses field measurements to condition model results in order to improve the predictions of observed solute spreading. Successful results were obtained with this technique, although (costly) site specific measurements are necessary. A somewhat different approach to heterogeneity of soil physical parameters was given by Jury [1982], who derived a transfer function model to calculate the distribution of solute travel times.

The studies concerning heterogeneity of porous media mainly involve variable soil hydraulic properties caused by spatially variable porosity, dispersion and hydraulic conductivity. Boekhold *et al.* [1990] have shown that chemical properties which play a role in the process of adsorption, such as pH and organic matter content, may show highly variable distributions. Studies concerning reactive solute transport with random sorption parameters were performed

Copyright 1993 by the American Geophysical Union.

Paper number 92WR01859.
0043-1397/93/92WR-01859\$05.00

by *van der Zee and van Riemsdijk* [1986, 1987], *Cvetkovic and Shapiro* [1990], *Destouni and Cvetkovic* [1991], *Jury et al.* [1986] and *Chrysikopoulos et al.* [1990]. *Cvetkovic and Shapiro* [1990] studied the mass arrival of transporting solute taking into account spatial variability of hydraulic conductivity, of linear adsorption coefficient, and of adsorption and desorption rate parameters. *Destouni and Cvetkovic* [1991] showed a double peak behavior for the mass arrival of solute into groundwater considering random hydraulic conductivity and random adsorption and desorption rate parameters. *Jury et al.* [1986] extended the transfer function model for solutes that undergo physical, chemical and biological transformations in heterogeneous systems. *Van der Zee and van Riemsdijk* [1987] used a random distribution of chemical parameters to simulate solute transport in a heterogeneous field. They found that variation of the retardation factor and the water velocity causes non-Fickian front shapes for the average field concentration front. *Chrysikopoulos et al.* [1990] studied the effect of a spatially variable retardation factor on linearly adsorbing one-dimensional solute transport, focusing on column scale heterogeneity.

Most studies reported here, describing soil physical or soil chemical heterogeneity, considered adsorption to be a linear process. However, as *Calvet et al.* [1980] showed for pesticides and *de Haan et al.* [1987] and *Boekhold et al.* [1990] have shown for heavy metals such as cadmium, adsorption may be nonlinear. For homogeneous media, *van der Zee* [1990b] derived an analytical solution for the limited traveling wave for a two-site system with equilibrium linear adsorption for one site and nonequilibrium nonlinear adsorption for the other site. This analytical solution was adapted by *Bosma and van der Zee* [1992b] in order to describe solute transport subject to nonlinear adsorption and first-order decay. A first approach to model nonlinear adsorption and column scale heterogeneity was performed by studying the effect of two-layered soils on solute transport [*Bosma and van der Zee*, 1992a].

Our aim is to analyze the effect of chemical heterogeneity on solute transport. Although we are aware of the significance of heterogeneity of hydraulic properties, this is not included in this study. In order to obtain basic information about the effect of variable nonlinear adsorption on one-dimensional solute transport, variation of the flow velocity has been ignored. A random distribution of the adsorption coefficient has been used. The method of moments [*Aris*, 1956] is applied, to quantify the effect of heterogeneity on the front velocity and on the front shape. Numerically calculated front variances are compared with an analytically derived expression for the variance of a traveling wave. By studying the ensemble average front, the effect of different front-spreading mechanisms is analyzed.

THEORY

We consider a solute, subject to nonlinear equilibrium adsorption, transported in the z direction of a soil. Since no production or decay is assumed, the governing equation for local equilibrium assumption (LEA) valid is given by (for symbols see the notation section)

$$\theta \frac{\partial c}{\partial t} + \rho \frac{\partial s}{\partial t} = \theta D \frac{\partial^2 c}{\partial z^2} - \theta v \frac{\partial c}{\partial z} \quad (1)$$

assuming steady state flow. With adsorption expressed on a volumetric basis (i.e., $q = \rho s$), (1) can be rewritten as

$$\theta \frac{\partial c}{\partial t} + \frac{\partial q}{\partial t} = \theta D \frac{\partial^2 c}{\partial z^2} - \theta v \frac{\partial c}{\partial z} \quad (2)$$

For this study nonlinear adsorption is described by the Freundlich equation, an expression often used to characterize adsorption of heavy metals and organic compounds [*de Haan et al.*, 1987; *Calvet et al.*, 1980]. The Freundlich equation is given by

$$q = kc^n \quad 0 < n < 1 \quad (3)$$

Our aim is to study the transport of a solute through a chemically heterogeneous soil, where k is a random space function. First we describe the behavior of a solute subject to nonlinear adsorption in a homogeneous soil. Depending on the nonlinearity of adsorption, *van Duijn and Knabner* [1990] have shown that under certain conditions a traveling wave front develops in a homogeneous porous medium. These conditions are, for $c_0 > c_i$, that $q' > 0$ and $q'' < 0$, where primes denote differentiation with respect to c . Due to the nonlinearity of adsorption, lower concentrations experience a larger retardation than higher concentrations (if $0 < n < 1$ in the Freundlich equation (3)). Consequently, a relatively steep front develops as adsorption nonlinearity opposes the front-spreading effect due to pore scale dispersion. If both effects, due to nonlinear adsorption and due to pore scale dispersion, are of equal force, the front shape and front velocity remain constant. *Van der Zee* [1990b] and *van Duijn and Knabner* [1990] have given an analytical solution for the limiting ($t \rightarrow \infty$) front. *Van der Zee* [1990b] and *Bosma and van der Zee* [1992a] have shown that in practice the traveling wave solution is already valid after short displacement times.

The initial and boundary conditions used for the derivation of the analytical solution are given by

$$c(z, t) = 0 \quad z > 0 \quad t = 0 \quad (4a)$$

$$c(z, t) = c_0 \quad z = 0 \quad t > 0 \quad (4b)$$

Bosma and van der Zee [1992b] gave the transformation to describe the concentration with respect to a moving coordinate system by

$$\eta = z - (vt/R) \quad (5)$$

where R , the nonlinear front retardation factor, is

$$R = 1 + \frac{\Delta q(c)}{\theta \Delta c} \quad (6)$$

in which $\Delta c = c_0 - c_i$ and Δq is the corresponding change in amount adsorbed. When the traveling wave front has formed we have

$$c(\eta) = c(z, t); \quad q(\eta) = q(z, t) \quad (7)$$

The transformed boundary conditions for the infinite system are

$$c(\eta) = c_0 \quad \frac{dc}{d\eta} = 0 \quad \frac{dq}{d\eta} = 0; \quad \eta = -\infty \quad (8a)$$

$$c(\eta) = 0 \quad \frac{dc}{d\eta} = 0 \quad \frac{dq}{d\eta} = 0; \quad \eta = \infty \quad (8b)$$

The analytical traveling wave solution for (2)–(3) is given as

$$\bar{c}(\eta) = \frac{c(\eta)}{c_0} = \left\{ 1 - \exp \left[\frac{v(R-1)}{DR} \cdot (1-n)(\eta - \eta^*) \right] \right\}^{1/(1-n)} \quad \eta \leq \eta^* \quad (9a)$$

$$\bar{c}(\eta) = 0 \quad \eta > \eta^* \quad (9b)$$

where $\bar{c}(\eta)$ is the relative concentration ($0 \leq c \leq 1$). The reference value η^* was discussed by *van der Zee* [1990b]. For LEA valid and $c_i = 0$, η^* is given by [*Bosma and van der Zee*, 1992a]

$$\eta^* = -(G^* + L_d) \quad (10)$$

with the constant G^* equal to

$$G^* = L_d \left(\frac{\theta + kc_0^{n-1}}{(1-n)kc_0^n} \right) \int_0^{c_0} \ln [1 - c_0^{n-1}c^{1-n}] dc \quad (11)$$

In (10) and (11), L_d is the dispersivity (equal to D/v , assuming no molecular diffusion).

With (9)–(11) it is possible to describe transport of a solute subject to nonlinear adsorption in a homogeneous soil. In order to quantify effects of several variables (e.g., degree of nonlinearity, dispersivity) and to assess the effects of heterogeneity, the concentration distribution can be characterized in terms of spatial moments [*Valocchi*, 1989]. The K th moment that can be calculated to analyze the concentration front moving in the z direction is defined as

$$M_K = \int_{-\infty}^{\infty} z^K f(z) dz \quad (12)$$

where $f(z)$ is the probability density function (pdf) of travel distance. To characterize the downward moving front with respect to the average front position, the K th central moment is defined as

$$M_K^c = \int_{-\infty}^{\infty} (z - \mu)^K f(z) dz \quad (13)$$

where μ is the first moment (M_1) given by (following (12))

$$\mu = M_1 = \int_{-\infty}^{\infty} z f(z) dz \quad (14)$$

In order to determine the moments M_K and M_K^c with (12)–(13), an expression for $f(z)$ is required. Similar to the linear adsorption case, $\bar{c}(z, t)$ is related to the cumulative probability or distribution function of travel distance z for a continuous injection as considered here. Hence, the derivative of $\bar{c}(z, t)$ with respect to z is related to the pdf of travel distance z for the nonlinear front. In particular,

$$f(z) = -\frac{\partial \bar{c}(z, t)}{\partial z} \quad (15)$$

The minus sign accounts for the descending front, i.e., our choice for the direction of the z coordinate, because the zeroth moment M_0 should be normalized to unity. We obtain for the moments of (12) and (13)

$$M_K = - \int_{-\infty}^{\infty} z^K \bar{c}'(z, t) dz \quad (16a)$$

$$M_K^c = - \int_{-\infty}^{\infty} (z - \mu)^K \bar{c}'(z, t) dz \quad (16b)$$

where primes denote spatial derivatives.

The defined moments physically describe a concentration front. The zeroth moment (M_0) gives the amount of dissolved solute present in the column. The first moment (M_1) denotes the average position of the front and, divided by time, quantifies the front velocity. The central moments are used to describe the front shape. The second central moment (M_2^c) gives the variance of the front s^2 , whereas the third central moment (M_3^c) and the fourth central moment (M_4^c) are related to the skewness and the kurtosis of the concentration distribution. For this study, we are mainly interested in the first moment (M_1 ; average front position) and the second central moment (M_2^c ; variance). Later, we will make use of the third and fourth central moments (M_3^c , M_4^c) to characterize the ensemble average concentration front of the flow domain.

If solute transport subject to nonlinear adsorption is considered, it is possible to derive an analytical expression for the variance of the front, provided (9) is valid, i.e., when k is constant and not a random space function (i.e., homogeneous porous medium). As mentioned earlier, a traveling wave is characterized by a constant front shape and a constant velocity. The constant front shape implies that the front variance is also invariant with time and depth. This suggests that an expression for the front variance s^2 can be derived that depends only on pore scale dispersion and on the degree of nonlinear adsorption. If, for convenience, we use the substitution $\bar{\eta} = \eta - \eta^*$ to rewrite (9) as

$$\bar{c}(\bar{\eta}) = [1 - \exp(P\bar{\eta})]^m \quad \bar{\eta} \in \langle -\infty, 0 \rangle \quad (17)$$

where

$$P = v(R-1)/DRm \quad (18)$$

$$m = 1/(1-n) \quad (19)$$

an expression for the variance $s_{\bar{\eta}}^2$ is derived with respect to the moving coordinate system $\bar{\eta}$. Because the front shape in terms of η is equal to the front shape in terms of z , and because the substitution $\bar{\eta} = \eta - \eta^*$ does not affect the front shape, we have the equivalence $s_{\bar{\eta}}^2 = s^2$. The variance $s_{\bar{\eta}}^2$ can be calculated according to

$$s_{\bar{\eta}}^2 = \langle (\bar{\eta} - \langle \bar{\eta} \rangle)^2 \rangle = \langle \bar{\eta}^2 \rangle - \langle \bar{\eta} \rangle^2 \quad (20)$$

where $\langle \bar{\eta} \rangle$ denotes the expected value of $\bar{\eta}$, given by the first moment (M_1). With (15) we can evaluate $\langle \bar{\eta}^2 \rangle$ according to

$$\langle \bar{\eta}^2 \rangle = - \int_{-\infty}^0 \bar{\eta}^2 \bar{c}'(\bar{\eta}) d\bar{\eta} \quad (21)$$

with the integration limits given by $-\infty$ and 0, in view of the $\bar{\eta}$ domain $(-\infty, 0]$ defined in (17). The second term on the right-hand side of (20) can be computed as

$$\langle \bar{\eta} \rangle^2 = \left(- \int_{-\infty}^0 \bar{\eta} \bar{c}'(\bar{\eta}) d\bar{\eta} \right)^2 \quad (22)$$

It is not necessary to evaluate the derivative of the concentration front ($\bar{c}'(\bar{\eta})$) for (21) or (22) because these equations can be formulated as

$$\langle g(\bar{\eta}) \rangle = - \int_{-\infty}^0 g(\bar{\eta}) \bar{c}'(\bar{\eta}) d\bar{\eta} = - \int_{-\infty}^0 g(\bar{\eta}) d\bar{c}(\bar{\eta}) \quad (23a)$$

$$\langle g(\bar{\eta}) \rangle = - [g(\bar{\eta}) \bar{c}(\bar{\eta})]_{-\infty}^0 + \int_{-\infty}^0 \bar{c}(\bar{\eta}) dg(\bar{\eta}) \quad (23b)$$

where $g(\bar{\eta})$ is a function of $\bar{\eta}$ (e.g., $\bar{\eta}^2$ in (21) or $\bar{\eta}$ in (22)). This shows that the expected value of $g(\bar{\eta})$ can be evaluated directly from the concentration front, $\bar{c}(\bar{\eta})$. The integrations of (21)–(22) with $\bar{c}(\bar{\eta})$ given by (17) can only be performed analytically for integer values of m . This restricts the values for n to $n = (i + 1)/(i + 2)$ (with $i = 0, 1, \dots, \infty$). For other n values, (21) and (22) have to be calculated numerically. To derive a general expression for $s_{\bar{\eta}}^2$, considering only positive integer values for m , the expression for $\bar{c}(\bar{\eta})$ given by (17) can be written as a series according to

$$\bar{c}(\bar{\eta}) = 1 + \sum_{i=1}^m \alpha_i \exp(Pi\bar{\eta}) \quad (24)$$

with

$$\alpha_i = (-1)^i \frac{m!}{(m-i)!i!} \quad (25)$$

Integrating (21) and (22) from $\bar{\eta} = -\infty$ to 0 using (24)–(25), an expression for the variance s^2 of a traveling wave front can be derived from (20). The obtained result is given by

$$s^2 = s_{\bar{\eta}}^2 = - \frac{2}{P^2} \sum_{i=1}^m \frac{\alpha_i}{i^2} - \frac{1}{P^2} \left(\sum_{i=1}^m \frac{\alpha_i}{i} \right)^2 \quad (26)$$

with P , m , and α_i given by (18), (19) and (25), respectively. With (26), the variance of a traveling wave for a homogeneous column, $s_{\bar{\eta}}^2$, which is related to the thickness of the front, can be calculated. Note that $s_{\bar{\eta}}^2$ is determined only by m and by P , which represent nonlinear adsorption and pore scale dispersion, respectively. In agreement with the traveling wave concept, $s_{\bar{\eta}}^2$ is independent of space and time.

NUMERICAL PROCEDURE

Incorporation of Heterogeneity

In order to describe solute spreading in heterogeneous porous media one must account for the often irregular variation of transport and adsorption parameters [Mackay *et al.*, 1986a, b]. To study the effect of column scale heterogeneity on solute transport, the transport and adsorption parameters may be considered variable in the vertical direction. Bosma and van der Zee [1992a] have shown the effect of layering on solute transport with nonlinear adsorption.

Considering linearly and nonlinearly adsorbing layers, the layering order was found to be important in order to describe the downstream concentration front. Whereas a soil consisting of two different layers was considered [Bosma and van der Zee, 1992a], here it is our aim to show the effect of multilayered soils.

In accordance with van der Zee [1990a], only variation of the adsorption parameters was considered in order to describe the effect of chemical heterogeneity, whereas variation of physical parameters such as flow velocity and dispersivity is not taken into account. The latter effects have been studied by Dagan and Bresler [1979], Bresler and Dagan [1979, 1981, 1983] and Amoozegar-Fard *et al.* [1982]. In view of the often rather constant n value [de Haan *et al.*, 1987; Boekhold *et al.*, 1991], we have considered only the Freundlich adsorption coefficient k to be random, characterized by a probability density function (pdf). The variation of the adsorption coefficient k is given by a normal distribution $N(m_k, s_k^2)$. Similar to Black and Freyberg [1987] and Chrysikopoulos *et al.* [1990], who used a spatial correlation of their random variable, we assumed the Freundlich adsorption coefficient k to be spatially correlated according to the exponential autocorrelation function given as

$$r(\zeta) = \exp(-\zeta/\lambda) \quad (27)$$

where ζ is the separation distance, r is the autocorrelation and λ is the correlation scale.

To assess the effect of a spatially variable adsorption coefficient, Monte Carlo simulations were performed. The random columns were finely discretized with different values for the adsorption coefficient k at each node. The columns had a prescribed probabilistic structure and each column is considered an equally likely configuration for the actual spatial pattern of the adsorption coefficient. A one-dimensional random generator has been used to construct one-dimensional random fields of a normally distributed parameter with autocorrelation described by the first-order exponential autocorrelation function given by (27). Use was made of a generator, creating uncorrelated normally distributed random numbers. To improve the accuracy of the reproduction of the autocorrelation structure in the random columns, more points per correlation scale were generated than actually used in the numerical transport calculations. The remaining points were not considered during the rest of the calculations. This technique, used by Bellin [1991], has been shown to improve the results.

The variable adsorption coefficient at each discrete generation point is evaluated by

$$k = m_k + \varepsilon \quad (28)$$

where m_k is the average adsorption coefficient and ε is the random fluctuation of m_k with zero mean. With the fluctuations ε the autocorrelation of the adsorption coefficient can be created. Using the first-order exponential autocorrelation function, the adsorption coefficient k at node i is determined by node $i - 1$, i.e.,

$$k_i = \beta k_{i-1} + \varepsilon_{i-1} \quad (29)$$

where β is the autocorrelation coefficient for two subsequent generation points. The variance of the fluctuation of k , s_ε^2 , is determined by the variance of k , s_k^2 , and can easily be derived from (29) as

$$s_{\varepsilon}^2 = (1 - \beta^2)s_k^2 \quad (30)$$

With s_{ε}^2 it is possible to generate uncorrelated normally distributed random fluctuations with a zero mean, so that (29) can be used to generate a random field of k with a first-order exponential autocorrelation function. With (30) this exponential autocorrelation function can be derived as

$$r = \beta^{|\Delta z^*|} \quad (31)$$

where Δz^* is the distance between the generation points. Relating the correlation scale λ to β , (31) can be rewritten in terms of ζ according to (27). The expression is given as

$$\lambda = -1/\ln \beta \quad (32)$$

With the random generator 600 possible chemically heterogeneous soil columns were generated. At each generation point of each column the k value is determined by the expected value m_k and the fluctuation ε . If the discretization of the columns used for the numerical calculations is given by Δz , these columns are constructed by selecting the k value of every j th generation point, where j is given by $\Delta z/\Delta z^*$.

Solving Transport Equations

A numerical solution of (2)–(3) has been developed to perform the calculations with the 600 random columns. The numerical solution is based on a finite difference Crank-Nicolson approximation of (2) in combination with a Newton-Raphson iteration scheme. In order to prevent oscillation the increments in depth z and time t were chosen to satisfy the criteria for linear adsorption, given by *van Genuchten and Wierenga* [1974]. The discretization makes it possible to specify a different adsorption coefficient for each node. A first type boundary condition was used at the inlet of the column, whereas at the outlet a flux type boundary was imposed:

$$c = c_0 \quad z = 0 \quad t \geq 0 \quad (33a)$$

$$\frac{\partial c}{\partial z} = \text{finite} \quad z \rightarrow \infty \quad t > 0 \quad (33b)$$

The initial condition for the numerical calculations was

$$c = c_i \quad z > 0 \quad t = 0 \quad (34)$$

where c_i was taken negligibly small.

The analytical solution (9) was derived for a zero initial concentration. The numerical approximation for that case is involved, as, due to the infinite derivative of (3) with respect to c at $c = 0$, we must deal with a moving boundary problem. We have taken the initial concentration negligibly small (but not zero) for the numerical approximation. This yields small deviations from the solution method proposed by *Dawson and Wheeler* [1990] for the same problem. These deviations are, for the chosen parameter values and the present context, insignificant.

Discretization of the soil columns is required for the numerical approximation and the implementation of chemical heterogeneity. Preliminary calculations for homogeneous columns illustrated that discretization should be done with extreme care, as otherwise s^2 for the numerical approximation does not agree with s^2 evaluated analytically with (26).

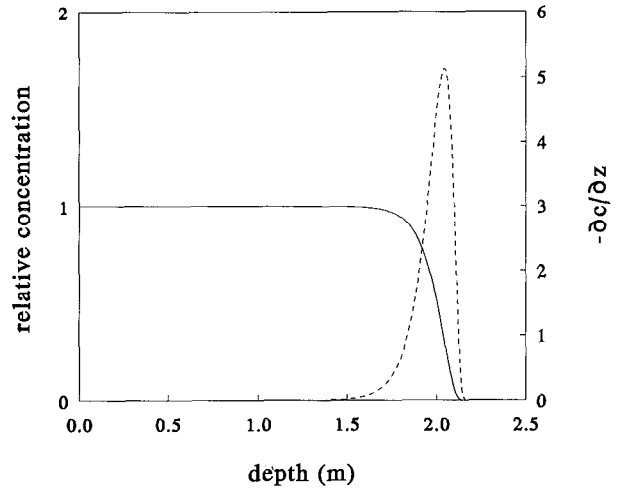


Fig. 1. Traveling wave front (solid line) with corresponding (negative) derivative (dashed line) at time $t = 42$ (for parameter values see Table 1).

Deviations arising from a wrong discretization were not always visible by comparing plots of front shapes, but were clearly visible by comparing limiting s^2 values ($t \rightarrow \infty$).

To evaluate the analytical solution given by (9) for a homogeneous soil column with a constant average adsorption coefficient k , the parameters R , η^* , and G^* need to be calculated. The parameter G^* , necessary to determine η^* in (10), can analytically be found for particular values of n . The integral in (15) has been solved analytically by *van der Zee* [1990b] for $n = (i + 1)/(i + 2)$ (with $i = 0, 1, \dots, \infty$). Here, we used a numerical integration of the integral in (11) to compute G^* and subsequently η^* .

Assessment of Spreading Mechanisms

Concentration distributions, calculated with the random columns using the numerical solution, give an indication of the effect of chemical heterogeneity. However, effects on the front shapes are difficult to distinguish by observing only the fronts. In a previous section we have derived an analytical expression for the variance of a traveling wave front in a homogeneous column. By computing the moments of the fronts in a chemically heterogeneous column and comparing these with the analytical moments of a homogeneous case, with the same spatially averaged k value for $0 < z \leq L$ for the heterogeneous and homogeneous column, the effect of heterogeneity can be demonstrated more clearly. The adsorption coefficient k determines the front shape and the front velocity (through retardation factor R). Hence, randomness of k causes a variation in both front shape and front velocity. Consequently, a numerical calculation of the moments described by (16) is necessary. The nonlinearity of adsorption causes steep fronts which may limit the accuracy of the numerical computation of the moments due to a lack of points between $\bar{c} = 1$ and $\bar{c} = 0$. Using a rational function interpolation method to interpolate between the calculated points of the fronts, we ensured a sufficiently large number of points to define the fronts. Consequently, the moments can be calculated numerically with the trapezoidal rule for integration. Figure 1 shows for a homogeneous column the traveling wave front with its related density function of z , \bar{c}' .

The dashed line in Figure 1, representing \bar{c}' , clearly has a non-Gaussian shape. The asymmetry of the front is due to the opposing effects of adsorption nonlinearity and of dispersion. Besides the asymmetric shape the non-Fickian behavior is also clear from the time and spatial independence of the front shape for the homogeneous column considered in Figure 1.

Incorporation of heterogeneity of the adsorption coefficients causes several mechanisms to play a role in solute spreading. These spreading mechanisms can be characterized as follows: (1) thickness of the individual traveling wave front; (2) column scale heterogeneity of the adsorption coefficient; and (3) different average retardation factors for an ensemble consisting of all columns.

The thickness of the individual traveling wave front can be assessed by considering a homogeneous column. The front width due to dispersion and, in this case, nonlinear adsorption, may play a role in all transport cases considered in this study. If, however, an individual heterogeneous column is taken into account, both thickness of the individual front and column scale heterogeneity play a role in solute spreading. The front velocity and front variance give an impression of the impact of the heterogeneity of the adsorption coefficient. Averaging over all realizations of the velocity and variance, both as a function of depth, yields the expected behavior of a heterogeneous column.

Additionally, an average front can be considered, representing an ensemble average front, assuming that the flow domain consists of an ensemble of parallel vertical random columns. In addition to the first two spreading mechanisms, extra spreading of the ensemble average front is caused by the variable average retardation factors for different columns. The latter spreading mechanism is caused by the numerical generation of the random columns. The fluctuation imposed on the mean value of the adsorption coefficient causes slightly different average adsorption coefficients for each column. Note that the effect of the third spreading mechanism decreases as the column length increases, because the bias in the column average k decreases with increasing number of generated points.

Parameter Values

For the simulations and analytical calculations of solute transport through chemically heterogeneous soils, we have chosen to calculate transport of cadmium. *De Haan et al.* [1987] have shown that contaminants like copper and cadmium show Freundlich adsorption behavior, and parameter values were available for Cd from *van der Zee* [1990b]. We have simulated transport of Cd with an initial concentration of 0 mol m^{-3} and a feed concentration of 0.02 mol m^{-3} . The flow parameters were kept constant in this study with the volumetric water content $\theta = 0.445$, bulk density $\rho = 1350 \text{ kg m}^{-3}$, dispersivity $L_d = 0.03 \text{ m}$, velocity $v = 1.9 \text{ m yr}^{-1}$, and consequently the dispersion coefficient $D = 0.057 \text{ m}^2 \text{ yr}^{-1}$. Of the chemical parameters with respect to which we have assumed n to be nonrandom, for Cd, $n = 0.65$. In agreement with *Chardon* [1984] and *de Haan et al.* [1987], the n value is relatively insensitive for soil type differences.

The random correlated fields of k were generated with an average m_k of 4.4, with a variance s_k^2 of 0.8. This results in a coefficient of variation CV of 0.2. This value is in a likely range, as shown by, e.g., *Boekhold et al.* [1990, 1991]. The

TABLE 1. Parameter Values

| Parameter | Value |
|--|----------------------|
| θ | 0.445 |
| ρ , kg m^{-3} | 1350 |
| l , m | 4 |
| v , m yr^{-1} | 1.9 |
| L_d , m | 0.03 |
| D , $\text{m}^2 \text{ yr}^{-1}$ | 0.057 |
| c_0 , mol m^{-3} | 0.02 |
| c_i , mol m^{-3} | 0 |
| m_k , $\text{mol}^{1-n} \text{ m}^{3(n-1)}$ | 4.4 |
| s_k^2 , $\text{mol}^{2-2n} \text{ m}^{6(n-1)}$ | 0.8 |
| n | 0.65 |
| λ , m | 0.22 |
| m_k^* , $\text{mol}^{1-n} \text{ m}^{3(n-1)}$ | 4.2 |
| Δz , m | 2.2×10^{-2} |
| Δz^* , m | 2.2×10^{-3} |

average k value gives an average retardation factor R of 40; however, the CV of R is not equal to the CV of k . The correlation scale used for the random fields was $\lambda = 0.22 \text{ m}$, denoting that the values of the adsorption coefficient may be considered to be uncorrelated for separation distances larger than 0.22 m . For the generation of the random columns Δz^* was $2.2 \times 10^{-3} \text{ m}$, creating 100 points per correlation scale. The node distance for the numerical calculations, Δz , was chosen to be $2.2 \times 10^{-2} \text{ m}$, which corresponds to 10 nodes per correlation scale. Consequently, this corresponds to a correlation scale of $\lambda = 10\Delta z$. The parameter values used for the transport calculations are summarized in Table 1.

RESULTS AND DISCUSSION

Homogeneous Column

In order to show the effect of nonlinear adsorption, Figure 2 gives the fronts and the related variances of the fronts, for cases with linear and nonlinear adsorption. For Figure 2 only analytical solutions have been used. Earlier research has given evidence of the appropriateness of the used analytical solutions [*Lapidus and Amundsen*, 1952; *van der Zee*, 1990b]. The traveling wave fronts of Figure 2 have been calculated with (9), whereas for the case with linear adsorp-

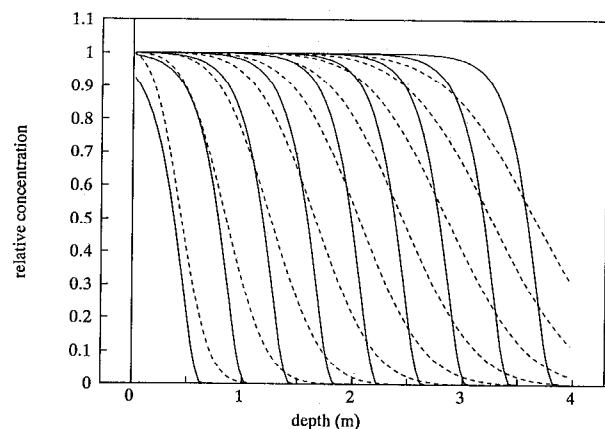


Fig. 2. Analytically calculated fronts for nine times $t = i\Delta t$ ($i = 1, 2, \dots, 9$; $\Delta t = 8.4$) for case with nonlinear adsorption and linear adsorption. Solid line: traveling wave solution (9). Dashed line: linear adsorption solution (35).

tion use was made of a solution given by *van Genuchten and Alves* [1982], i.e.,

$$\bar{c}(z, t) = \frac{1}{2} \operatorname{erfc} \left(\frac{R_1 z - vt}{2(DR_1 t)^{1/2}} \right) + \frac{1}{2} \exp \left(\frac{vz}{D} \right) \operatorname{erfc} \left(\frac{R_1 z + vt}{2(DR_1 t)^{1/2}} \right) \quad (35)$$

where, in this case, R_1 was set equal to R .

From Figure 2 can be seen that the shape and velocity of the traveling wave front become constant during the solute displacement. The analytical solution given by (9), used for the calculations of the traveling wave fronts of Figure 2, has been derived for the limiting case ($t \rightarrow \infty$), and is therefore not valid for early displacement times. *Van der Zee* [1990b] has shown that although small deviations occur between the analytical solution and the numerical approximation upon entry of the solute into the column, the solution is quickly applicable. The analytical solution assumes an instantaneous front shape with a variance to be calculated with (26), whereas in practice the front shape starts as a block front that converges to the actual traveling wave. This effect causes the deviating front depths of the concentration fronts at early displacement times in Figure 2. At larger displacement times these deviations of the average front depths disappear.

In Figure 3 we show how the front velocity (related to the first moment) and the variance (second central moment) of

the numerical solution approach the constant values of the analytical traveling wave solution. The velocity of the analytical traveling wave is determined with the retardation factor, whereas the analytical variance is computed with (26). For comparison, we have divided the velocities and variances by the analytical values, which yields relative quantities. Figure 3a shows that the actual front starts with a velocity of zero, but rapidly approaches the velocity calculated by the analytical solution. From Figure 3b it can be seen that, compared with the front velocity, more time is necessary for the numerical solution to obtain the exact thickness of the traveling wave front. However, it is clear that although the traveling wave solution is derived for $t \rightarrow \infty$, the solution is applicable at earlier times. In fact, we will demonstrate that the reaction time of the front shape is quick enough to show differences due to a spatially variable adsorption coefficient k in the random columns.

Heterogeneous Column

An analysis as given above of the front shape and front velocity of a concentration front characterized by a traveling wave is applicable to homogeneous columns. In practice, however, soils are physically and chemically heterogeneous. Looking at a single realization, randomly selected from the 600 columns with normally distributed adsorption coefficient k , we are able to obtain information about the effect of heterogeneity of nonlinear adsorption. The selected profile is a feasible representation of the ensemble of columns generated with m_k and s_k^2 , as given in a previous section. The distribution of the adsorption coefficient k with its related statistics (mean, standard deviation and autocorrelation) is given in Figure 4. Additionally, Figure 4b shows the first-order autocorrelation function used as input for the generation of the random columns. The distribution of the adsorption coefficient k has been used to numerically calculate the solute fronts. Subsequently, we have used the average adsorption coefficient of this realization, m_k^* , to compare the numerically calculated fronts with analytically calculated fronts for the homogeneous case.

The results given in Figure 5 show that the chemical heterogeneity causes a spatially variable rate of solute transport. Due to a series of high peaks of the adsorption coefficient in the top part of the column (Figure 4a), the retardation factor increases, which causes a lower solute velocity until $z = 2$ m. An ensuing series of low adsorption parameters causes an increase of the front velocity. At the end of the column the numerical fronts coincide with the analytical fronts. This is caused by the averaging procedure of the adsorption coefficient necessary for the analytical solution. Consequently, at $z = 4$ m both cases have experienced the same total retardation.

The numerical and analytical fronts of Figure 5 give a qualitative view of the effect of chemical heterogeneity. In fact, in Figure 5 only the effect on the front velocity is visible, whereas differences in front shapes cannot be detected. Figure 6 gives the relative velocity of the front, calculated with the first moment, and the relative variance of the front, represented by the second central moment. For reasons of comparison we have chosen to represent the velocity and variance as relative quantities. Apparently, the front shape is also sensitive for the variable adsorption coefficient. The variance and velocity both have peaks at

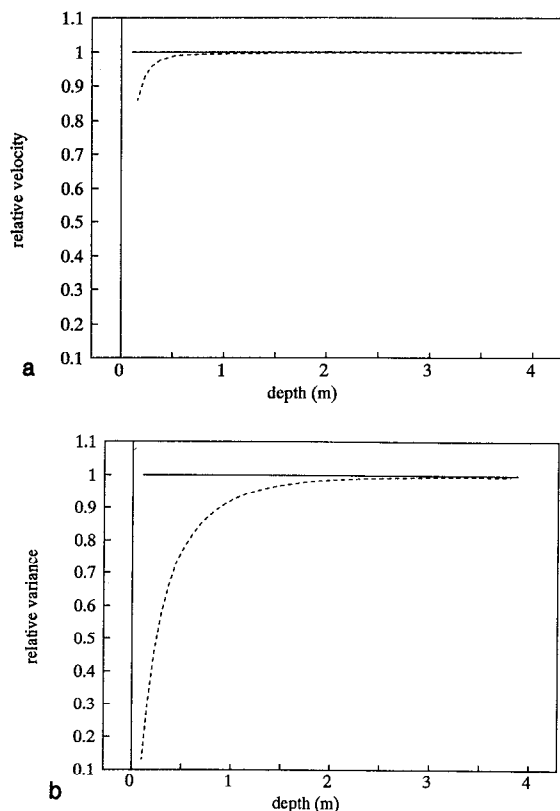


Fig. 3. (a) Relative front velocity and (b) relative front variance of numerically calculated transport through homogeneous columns. Dashed lines: numerically calculated relative velocities and variances. Solid lines: analytically calculated relative velocity and variance.

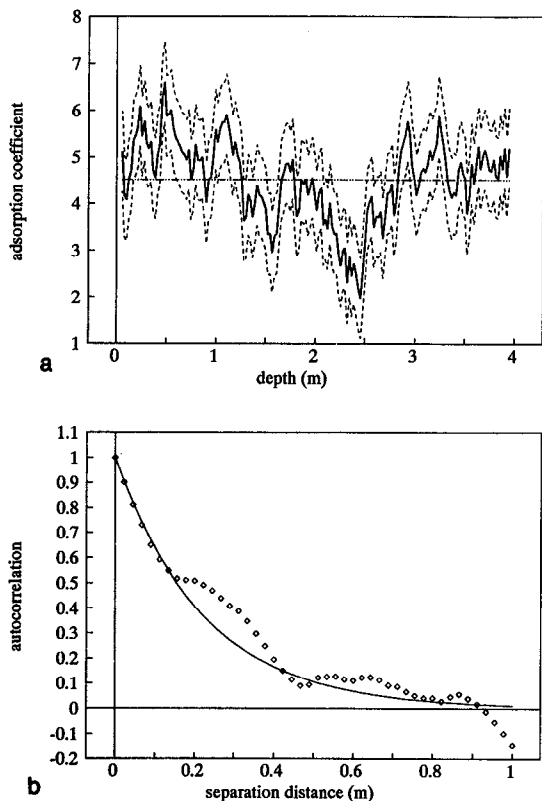


Fig. 4. (a) Spatial distribution and (b) autocorrelation (diamonds) of the adsorption coefficient of a single realization. In Figure 4a, the dashed-dotted line denotes mean value, and the dashed line denotes distribution plus and minus standard deviation. In Figure 4b, the solid line denotes first-order autocorrelation used as input for generation of random columns.

corresponding depths, indicating that a high adsorption coefficient causes steeper fronts. This observation agrees with *van der Zee* [1990b], who showed that the effect of nonlinearity of adsorption is larger when the adsorption coefficients are larger. Hence a steeper traveling wave front results. Figures 5–6 demonstrate that describing the concentration front in terms of moments can be very useful. Influences of a variable adsorption coefficient on the front shape are invisible in Figure 5, whereas the variance, with its

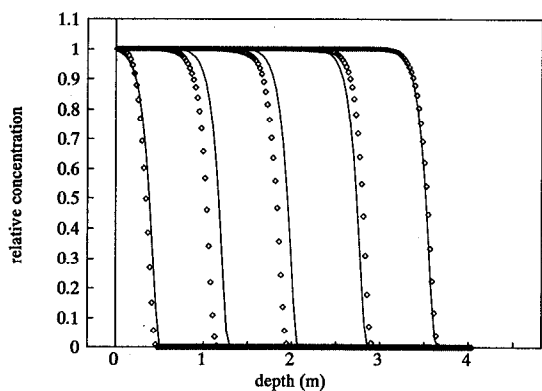


Fig. 5. Fronts for five times $t = i \cdot \Delta t$ ($i = 1, 2, \dots, 5$; $\Delta t = 16.8$) through a chemically heterogeneous column of an individual realization. Solid line: analytical traveling wave solution with average adsorption coefficient. Diamonds: numerically calculated fronts.

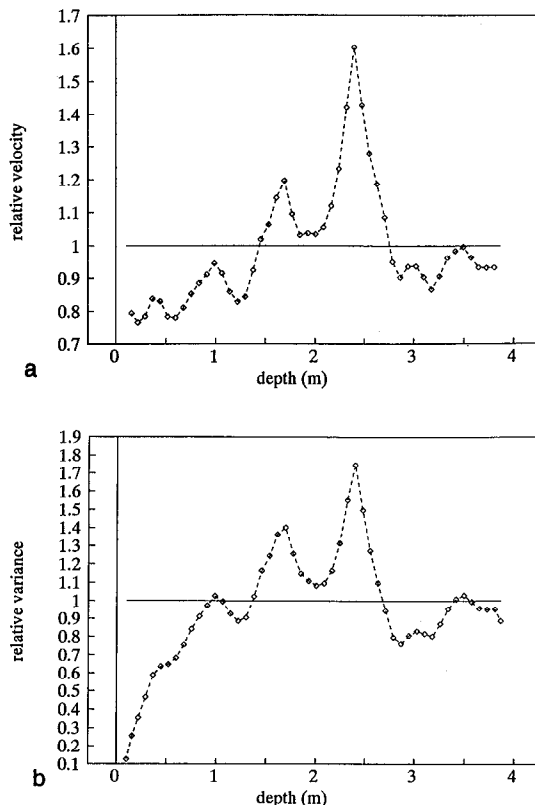


Fig. 6. (a) Relative front velocity and (b) relative front variance of numerically calculated transport through a heterogeneous column. Dashed lines with diamonds: relative velocities and variances. Solid lines: constant velocity and variance of homogeneous column with corresponding average adsorption coefficient.

high sensitivity, shows a clear variation of the front thickness. Similar to the variance of the homogeneous case, shown in Figure 3b, the variance of the heterogeneous realization needs more displacement time to approach the analytical value than the velocity. Nevertheless, the sensitivity of the front variance is high enough to react to the pattern of the variable adsorption coefficient, shown in Figure 4a.

A different way to show the effect of the spatially variable adsorption coefficient k on the concentration front is to compare the autocorrelation of the spatial distribution of the adsorption coefficient with the autocorrelation of the distribution of the front velocity and front variance. The autocorrelations of the adsorption coefficient k of the front velocity and of the front variance are given in Figure 7. It can be seen that all three correlations follow about the same course. The autocorrelation of the adsorption coefficient k at the lower separation distances is less than the autocorrelation of the other two quantities, indicating that at a short distance values of the adsorption coefficient are less similar than values of the velocity and variance. This can be seen from Figures 4–6 where the distribution of the adsorption coefficient k is shown to be highly variable, even at short distances. The distributions of the front velocity and front variance show a corresponding course, but are more smoothed, causing a decrease of the small-scale variability. The smoothing is due to the fact that a concentration front is spread out over a number of nodes, whereas the values of the adsorption coefficient are node specific. If a moving

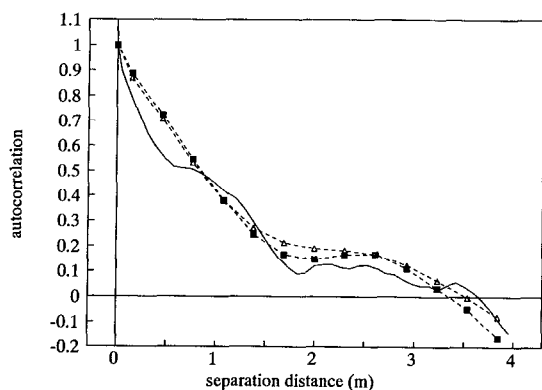


Fig. 7. Autocorrelations of adsorption coefficient (solid line), front velocity (dashed line with triangles), and front variance (dashed line with squares).

average of the adsorption coefficients k is calculated, the profile of k is more smoothed, corresponding to the distributions of the front velocity and front variance. The adsorption coefficient profile, calculated as a moving average, is shown in Figure 8a. Figure 8b demonstrates the corresponding autocorrelation of the moving average adsorption coefficient, compared with the autocorrelations of the front velocity and front variance. At lower separation distances the autocorrelation of the average adsorption coefficient has increased and corresponds to the autocorrelation of the front velocity and the front variance. The small-scale heterogeneity is reduced.

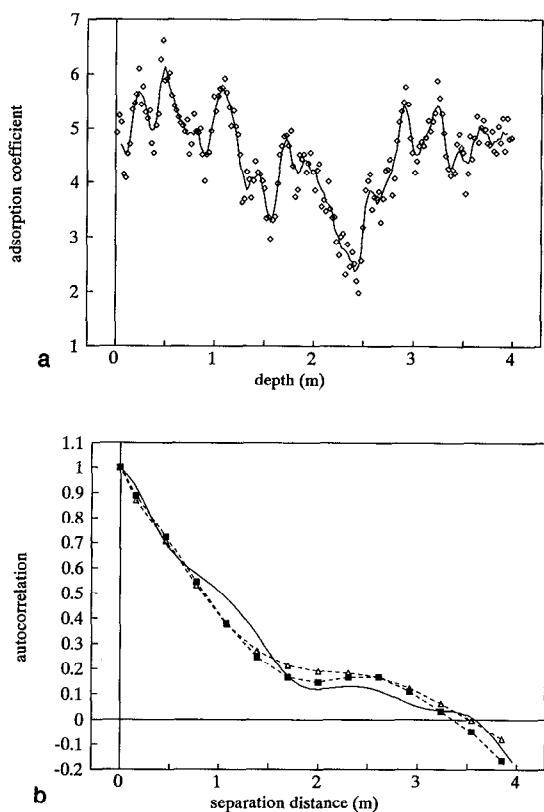


Fig. 8. (a) Moving average of the adsorption coefficient k , averaged over five nodes. (b) Autocorrelations of moving average adsorption coefficient (solid line), front velocity (dashed line with triangles), and front variance (dashed line with squares).

In general, it can be said that chemical heterogeneity of nonlinear adsorption causes deviations of the velocity and thickness of the traveling wave front. Figures 5–6 demonstrate that the heterogeneity has significant effects on single realizations of nonlinearly adsorbing solute transport. Values of front velocity and front variance are locally substantially higher than the analytical values calculated with an average adsorption coefficient. If, however, adsorption would be described as a linear process, the front variances would be much larger, due to the increasing thickness of the concentration front as displacement proceeds.

Expected Heterogeneous Column Behavior

Due to one-dimensional chemical heterogeneity the front shape and front depth can be highly variable. A single realization has been shown to give results deviating considerably from the homogeneous case with a nonvariable single-valued adsorption coefficient. The randomness of a single realization increases the uncertainty to make predictions concerning the arrival time and front thickness at a certain point. The best prediction of front velocity and front variance is the expected value of the two quantities. The expectation characterizes the effect of the spreading mechanism denoted by column scale heterogeneity. The spreading around the expected values is a measure of the possible deviations from the expected values.

The best available estimate for the expected value of the front velocity and front variance is obtained by averaging these quantities for all 600 random columns. The average velocity and average variance are given as a function of depth in Figure 9. Both quantities are represented as relative quantities with respect to the analytical value for the case of a homogeneous traveling wave solution. The latter was calculated with the average adsorption coefficient. As is shown in Figure 9, the averaging has a smoothing effect. The deviations from the analytical value are significantly smaller compared with a single realization (Figure 6). In fact, if an infinite number of columns were used, the average velocity and variance curves would increase smoothly, just like in Figure 3 (however, not necessarily to the same value). In Figures 3a and 3b the confidence intervals are not shown, for they are equal to about 1% of limiting velocity and variance, respectively. This proves convergence of the Monte Carlo calculations. Note that, corresponding to a single realization, the expected variance tends to a constant value, typical for a traveling wave. However, if adsorption were described as a linear process, the expected variance would increase continuously with depth.

Additionally, Figure 9 reveals that the spreading around the analytical velocity is smaller than the spreading around the analytical variance (compare different scales). Therefore, the expected velocity will not differ much from the analytical velocity of the homogeneous case. The average variance tends toward a value larger than the analytical variance of the traveling wave front. The fact that the expected value of the variance is not equal to the value calculated with average parameters can be visualized with the frequency distributions in Figure 10. Here, 8000 adsorption coefficients were randomly generated, following a normal distribution (Figure 10a). With the ensemble of normally distributed adsorption coefficients and constant values of n , θ and c_0 , normally distributed retardation factors have been computed according to

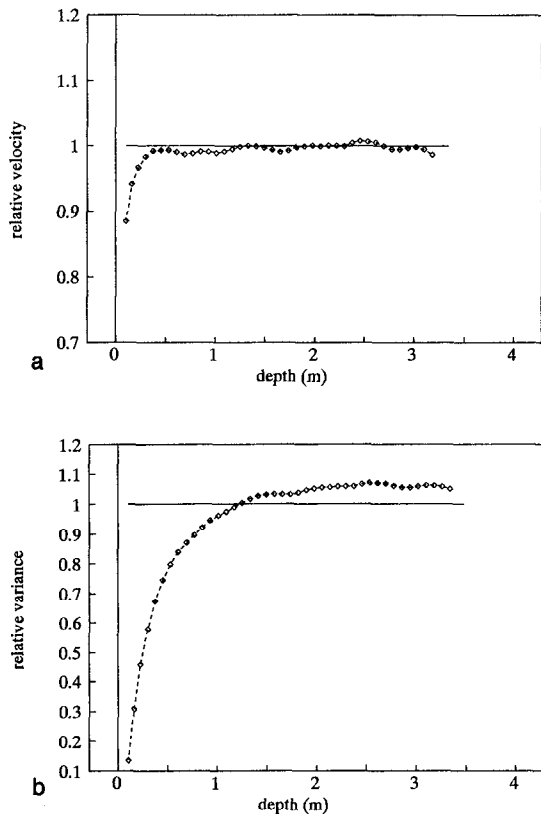


Fig. 9. (a) Averaged relative front velocity and (b) averaged relative front variance. Dashed lines: averaged relative velocities and variances. Solid lines: constant averaged relative velocity and variance for homogeneous columns with constant average adsorption coefficients.

$$R = 1 + \frac{k}{\theta} c_0^{n-1} \quad (36)$$

where k is the random variable. If, with a normally distributed R , the front variance is calculated with (26) a frequency distribution is produced with a non-Gaussian shape. The frequency distribution of the front variance is given in Figure 10b. The nonlinear relationship between variance and R in (26) causes the shape that differs from a normal distribution. The expected value in Figure 10b is larger than the median, calculated with the analytical solution (26) and shown as the solid line in Figure 9.

Ensemble Average Front

An extra effect of chemical heterogeneity can be studied by considering the ensemble average fronts of the 600 random columns. The ensemble average front represents an average front for a flow domain, consisting of an ensemble of parallel noninteracting soil columns. Representing a field in this manner was introduced by *Dagan and Bresler* [1979], and applied to a chemically spatial variable field by *van der Zee and van Riemsdijk* [1987] and *Destouni and Cvetkovic* [1991]. Considering the flow domain, we have a random distribution of the adsorption coefficient k in each column, combined with a spatial distribution of the average adsorption coefficient over the domain. The latter causes slightly different average retardation factors for each column, and therefore a variable flow domain of the transported solute.

Consequently, in some columns the solute will move more rapidly than in others.

Compared with the case of column scale heterogeneity, the extra front spreading mechanism due to the spatially variable retardation factor causes a different behavior of the ensemble average front. Whereas only two spreading mechanisms are present if column scale heterogeneity (individual front spreading and column scale heterogeneity) is considered, here we are dealing with three spreading mechanisms, which have been discussed previously.

In a previous section it has already been shown that for a homogeneous column the thickness of a traveling wave (the first spreading mechanism) can be calculated analytically with (26). Since the front shape is not much affected by column scale heterogeneity, (26) can also be used as an estimation for the front thickness in heterogeneous columns.

To study the spreading due to column scale heterogeneity and due to the spatially variable retardation factor (second and third spreading mechanisms), results are given in Figure 11 of the ensemble average fronts, with corresponding variance, of the heterogeneous columns and of the homogeneous columns with variable average retardation factors. Of the above mentioned spreading mechanisms, the column scale heterogeneity does not apply to the case with homogeneous columns. In the flow domain with homogeneous columns, the ensemble average fronts have been calculated with traveling wave fronts computed with different average adsorption coefficients.

The first effect visible in Figure 11a is, in contrast with a traveling wave front, that the ensemble average front has a continuously spreading character. Figure 11b verifies this with

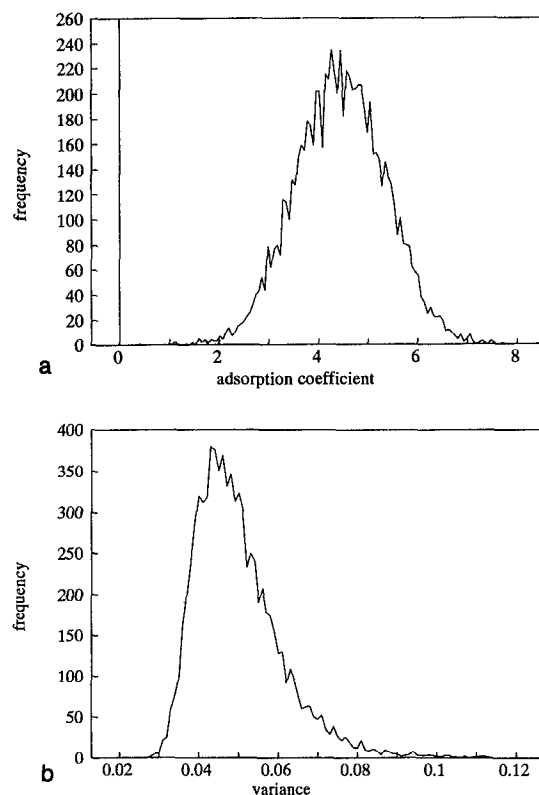


Fig. 10. Frequency distributions of (a) 8000 adsorption coefficients, and (b) 8000 corresponding variances, analytically calculated with (26).

a continuously increasing variance. This can be explained by the variable retardation factor at each column, which causes a variable velocity field of the transported solute. Consequently, during displacement time, the front will spread continuously.

A different effect, visible in Figure 11a, is that there is good agreement between the ensemble average fronts of the heterogeneous columns and the fronts of the homogeneous columns with variable average retardation factors. This implies that the second spreading mechanism, the column scale heterogeneity, is of minor importance when considering ensemble average fronts. The spatial distribution of the retardation factor over the different columns predominates over the effect of front spreading. From Figure 11b can be seen that at early displacement times the effect of the average retardation factors of the different columns is still small. The variance of the ensemble average front of the homogeneous columns with variable average retardation factor is equal to the variance of the individual traveling wave, whereas the thickness of the ensemble average front of the heterogeneous columns is initially zero. At larger displacement times the effect of column scale heterogeneity becomes relatively less important and, consequently, the relative effect of the variable average retardation factor becomes larger. The difference between the variances of the ensemble average front of the heterogeneous columns and the homogeneous columns hardly changes, whereas the absolute value of the variances continuously increases. Note that Figure 11b again justifies the use of moments. The effect of column scale heterogeneity can be made clearly visible.

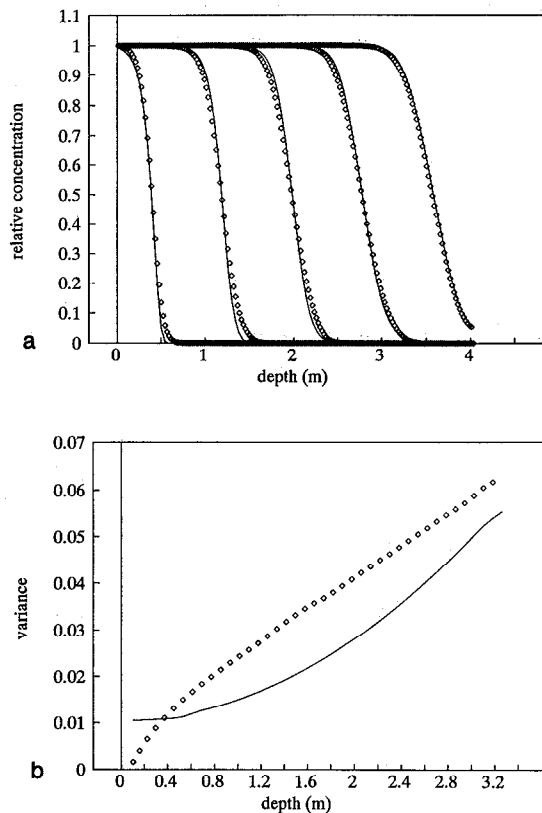


Fig. 11. (a) Ensemble average fronts and (b) corresponding variances. Solid lines: ensemble average fronts and variances of 600 homogeneous columns with variable averaged adsorption coefficient (ignoring column scale heterogeneity). Diamonds: ensemble average fronts and variances of 600 heterogeneous columns.

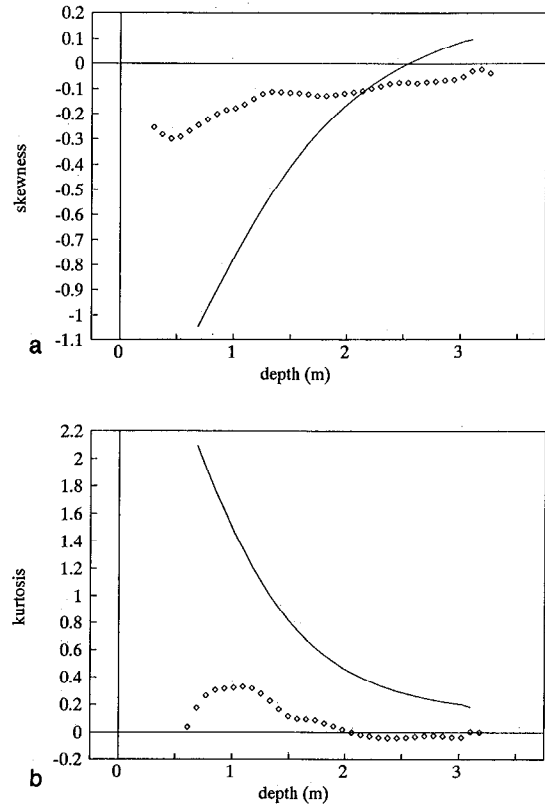


Fig. 12. (a) Skewness and (b) kurtosis of the ensemble average fronts. Solid lines: properties of ensemble average fronts of 600 homogeneous columns with variable average adsorption coefficients. Diamonds: properties of ensemble average fronts of 600 heterogeneous columns.

In addition to the second central moment, use can be made of the third and fourth central moments to assess the shape of the ensemble average concentration front. The third central moment of a concentration front can be used to quantify the skewness of the distribution function, $\bar{c}'(z, t)$. The fourth central moment is related to the kurtosis of the distribution function. The kurtosis measures the peakedness or flatness of the distribution. In order to compare the distribution functions, both skewness and kurtosis are non-dimensional quantities with a value of 0 for normal distributions.

Figure 12 shows the skewness and kurtosis for the ensemble average front of 600 heterogeneous columns and for the ensemble average front of 600 homogeneous columns with different average adsorption coefficients. In Figure 12a we see that the skewness of the ensemble average front for the homogeneous columns with different average adsorption coefficients approaches a value just above the value characterizing a normal distribution. The skewness increases from a negative value, which represents the skewness of a single traveling wave front. The negative skewness is due to a stronger adsorption of the lower concentrations compared to adsorption of the higher concentrations. This causes the front to be steeper at low concentrations, resulting in a negatively skewed distribution function $\bar{c}'(z, t)$. The skewness of the ensemble average front of the heterogeneous columns shows similar results. In the course of displacement the value of the normal distribution is approached. At $t = 0$ the solution of the heterogeneous column starts as a block

front, causing a lesser negative skewness at early displacement time compared with the skewness of the ensemble average front for the homogeneous columns. The approach to the value 0 of the fronts of the heterogeneous columns clearly demonstrates a normal behavior of the ensemble average front.

The normal behavior of the ensemble average front is verified by Figure 12b, which demonstrates the kurtosis of the concentration distributions. Corresponding to Figure 12a, the kurtosis for the ensemble average front calculated with homogeneous columns with different average adsorption coefficients approaches a value just above the normal value. The approach starts at the characteristic kurtosis of a single traveling wave. The kurtosis of the ensemble average front calculated with the heterogeneous columns shows a behavior corresponding to a normal distribution.

The discrepancy between the behavior of the ensemble average front of the homogeneous columns and a normal distribution (illustrated with skewness and kurtosis) can be attributed to the front shape of an individual traveling wave front. The steepness of the downstream part of the regular traveling wave causes the deviations of the average front from 0 in Figure 12 (horizontal solid line). The ensemble average front of the heterogeneous columns shows a normal behavior due to averaging out of the irregularities of the individual fronts which develop in the heterogeneous columns (see Figure 6).

If column scale heterogeneity is ignored, it is possible to derive an analytical approximation for the ensemble average front. This approximation can be obtained by adjusting the analytical solution for Fickian-type transport given by (35). If transport with linear adsorption in a homogeneous medium is considered, (35) can be rewritten in terms of the first moment (average position) and the second central moment (variance) of the front. To use (35) in order to describe the ensemble average front we have to account for the extra spreading due to the thickness of the individual traveling wave front.

If v^* is defined as the ensemble average front velocity ($v^* = v/R$), the mean position m_z and the variance s_z^2 of the ensemble average front can be given as

$$m_z = m_{v^*} t \quad (37a)$$

$$s_z^2 = s_{\eta}^2 + (s_{v^*} t)^2 \quad (37b)$$

where s_{η}^2 is the variance of an individual traveling wave, given by (26). To arrive at (37) we have assumed that $1/R$ is normally distributed if R is normally distributed, which in general is only valid if the coefficient of variation of R is small. With (37) the analytical approximation for the ensemble average front can be derived from (35) as

$$\bar{c}(z, t) = \frac{1}{2} \operatorname{erfc} \left(\frac{z - m_z}{s_z \sqrt{2}} \right) + \frac{1}{2} \exp \left(\frac{2m_z}{s_z^2} z \right) \operatorname{erfc} \left(\frac{z + m_z}{s_z \sqrt{2}} \right) \quad (38)$$

With Fickian-type transport (linear adsorption) in homogeneous columns, the variance s_z^2 is not given by (37b), but can be written as

$$s_z^2 = 2Dt/R_t \quad (39)$$

Equation (39) shows that s_z^2 increases linearly with time t . However, for a spatially variable retardation factor, the

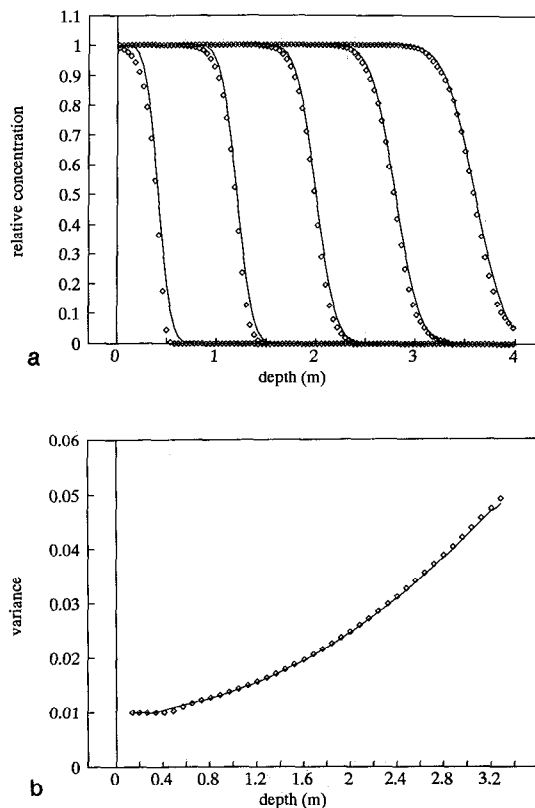


Fig. 13. (a) Analytical approximation of ensemble average front and (b) corresponding variances, ignoring column scale heterogeneity. Solid lines: analytical approximation (38) and variances of ensemble average fronts. Diamonds: ensemble average fronts and variances of 600 homogeneous columns with variable average adsorption coefficient.

variance s_z^2 increases with t^2 , as can be seen in (37b). This can be visualized in Figure 11b, where a parabolic course is clearly visible.

To show the applicability of (38), Figure 13 gives the results of the ensemble average front of the homogeneous columns with variable average retardation factors, approximated by the adjusted analytical solution. The corresponding variances are shown as well. Despite the assumption that $1/R$ is normally distributed the agreement is good, although at early displacement times the ensemble average front has the shape of a traveling wave, which cannot be described adequately by a Fickian-type front.

In the above considered case, column scale heterogeneity was ignored, because the distribution of the average retardation factor produced dominant effects. However, neglecting column scale heterogeneity may not always be justified. In the case with heterogeneous columns, an extra term needs to be added to (37b) to account for the column scale heterogeneity. Although this term is unknown, it will be dependent on s_k^2 , the variance of the adsorption coefficient within a single column. Whereas at large displacement times ($t \rightarrow \infty$) the spreading of the ensemble average front will be dominated by the $(s_{v^*} t)^2$ term, this term will show less dominating effects in cases with large column scale heterogeneity and small differences between columns if the limiting situation has not yet been reached.

The effect of column scale heterogeneity can be demonstrated more clearly if we consider the 600 randomly gener-

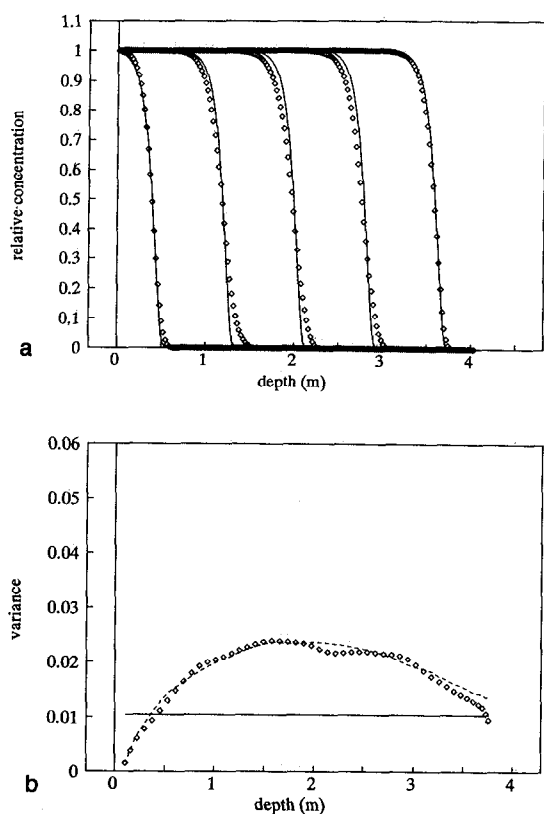


Fig. 14. (a) Ensemble average fronts omitting the variable average retardation factor and (b) corresponding variances. Solid lines: traveling wave fronts and variance with m_k . Dashed line (Figure 14b): difference between the variances of Figure 11b added to variance of individual traveling wave. Diamonds: ensemble average fronts and variances of 600 heterogeneous columns with equal average adsorption coefficients.

ated heterogeneous columns with adjusted adsorption coefficients, so that the average front retardation factors are equal in all columns. At each node the adsorption coefficients have been multiplied with a column-specific factor, in order to equalize the average adsorption coefficients of all columns. Therefore, $m_{v*} = v/R$, where R is constant and $s_{v*}^2 = 0$. In this situation two front-spreading mechanisms are significant: the thickness of the individual traveling wave and the column scale heterogeneity of the adsorption coefficient. The ensemble average fronts with the corresponding variances are given in Figure 14. Figure 14a shows how the ensemble average front attains a shape, deviating from the Freundlich traveling wave, but remaining constant during the transport process. The continuous spreading of the ensemble average front of Figure 11a is removed and the resulting front demonstrates a significant symmetric shape. At the end of the column the front approaches a Freundlich traveling wave front, because at that point all columns have experienced the same average adsorption coefficient.

In Figure 14b the dashed line is based on the difference of the variances of the ensemble average front with the three front-spreading mechanisms and the variances of the ensemble average front with the homogeneous columns with variable retardation factor, both given in Figure 11b. This difference represents the spreading due to the spatial distribution of the adsorption coefficients within the columns. If the difference between the two variances of Figure 11b is

added to the expected thickness of the traveling wave, s_{η}^2 , these two added spreading mechanisms approach the variances of the ensemble average front of Figure 14a. Figure 14b shows that the different front-spreading mechanisms are completely additive.

The procedure of omitting the variability of the average retardation factors demonstrates a few valuable aspects. First, it can be seen that, in this situation, the variance of the ensemble average front tends to a constant value. At the end of the column the thickness of the front decreases, which is due to the fact that at that point all columns have experienced the same average retardation factor. At the beginning of the column the curves show an equal course, for this part mainly represents the approach of the actual individual fronts to the individual traveling wave. The internal heterogeneity still has little effect.

Figure 14b, compared with Figure 11b, also gives the significance of the variance due to column scale heterogeneity. It can be seen that this front-spreading mechanism is quite relevant, although, after longer displacement times, variation of the different retardation factors among columns will dominate the front-spreading process.

CONCLUSIONS

We have studied the effect of chemical heterogeneity on solute transport in one-dimensional soil columns. The heterogeneity was obtained by assuming a random variation of the Freundlich adsorption coefficient with depth. A normal distribution in combination with exponential autocorrelation was assumed. The method of moments was used to show the effect of chemical heterogeneity on the front velocity and on the front variance. This method was proven to be very valuable, for differences in front shape could be made clearly visible. Considering a homogeneous column, an analytical expression was derived for the front variance, which is, due to nonlinear adsorption, nonvariable with space and time. For a single realization, chemical heterogeneity has a significant effect. The front velocity and front variance may show large deviations from the case with average adsorption coefficient. The expected values of the front velocity and front variance, calculated as average values from 600 randomly generated columns, show a more smoothed character compared with single realizations. The front velocity shows less spreading around the case calculated with average adsorption coefficient than the front variance. The nonlinear character of the calculations causes the deviations from the case with average parameters. Considering the ensemble average front, it was shown that three front-spreading mechanisms play a role. First, the thickness of the individual fronts causes spreading, followed by an effect of the internal variation of the adsorption coefficient in the individual columns. With time, the effect of different average retardation factors of different columns increases and dominates the front spreading. It was shown that the latter spreading mechanism causes a front to spread proportionally to t^2 . Due to the time dependency, the internal variation of the adsorption coefficient can, in some cases, be insignificant. Nevertheless, the steep fronts caused by nonlinear adsorption, in contrast with the continuously spreading fronts caused by linear adsorption, prove the importance of the characterization of the adsorption process.

NOTATION

| | |
|---------------|--|
| c | concentration, mol m ⁻³ . |
| c_0 | feed concentration, mol m ⁻³ . |
| c_i | initial concentration, mol m ⁻³ . |
| \bar{c} | relative concentration. |
| Δc | concentration difference, mol m ⁻³ . |
| CV | coefficient of variation. |
| D | pore scale dispersion coefficient, m ² yr ⁻¹ . |
| f | probability density function. |
| g | function. |
| G^* | constant. |
| k | nonlinear adsorption coefficient, mol ¹⁻ⁿ m ³⁽ⁿ⁻¹⁾ . |
| l | column length, m. |
| L_d | dispersivity, m. |
| m | parameter. |
| m_k | average adsorption coefficient, mol ¹⁻ⁿ m ³⁽ⁿ⁻¹⁾ . |
| m_k^* | average adsorption coefficient of a single realization, mol ¹⁻ⁿ m ³⁽ⁿ⁻¹⁾ . |
| m_{v^*} | average ensemble average front velocity, m yr ⁻¹ . |
| m_z | average position of ensemble average front, m. |
| M_K | K th moment. |
| M_K^c | K th central moment. |
| n | Freundlich sorption parameter. |
| q | adsorbed amount (volumetric basis), mol m ⁻³ . |
| Δq | change in q , mol m ⁻³ . |
| P | parameter. |
| r | autocorrelation coefficient. |
| R | nonlinear retardation factor. |
| R_l | linear retardation factor. |
| s | adsorbed amount (mass basis), mol kg ⁻¹ . |
| s^2 | variance (second central moment). |
| s_k^2 | variance of adsorption coefficient, mol ²⁻²ⁿ m ⁶⁽ⁿ⁻¹⁾ . |
| $s_{v^*}^2$ | variance of ensemble average front velocity, m ² yr ⁻² . |
| s_z^2 | variance of ensemble average front, m ² . |
| s_ξ^2 | variance of the random fluctuation, mol ²⁻²ⁿ m ⁶⁽ⁿ⁻¹⁾ . |
| s_η^2 | variance of traveling wave front, m ² . |
| t | time, yr. |
| v | velocity, m yr ⁻¹ . |
| v^* | ensemble average front velocity, m yr ⁻¹ . |
| z | depth, m. |
| Δz | node distance for numerical calculations, m. |
| Δz^* | distance between generation points for random columns, m. |
| α_i | parameter. |
| β | autocorrelation coefficient for two subsequent nodes. |
| ε | random fluctuation of adsorption coefficient k , mol ¹⁻ⁿ m ³⁽ⁿ⁻¹⁾ . |
| ζ | separation distance, m. |
| η | transformed coordinate, m. |
| η^* | reference point value of η , m. |
| $\bar{\eta}$ | parameter, equal to $\eta - \eta^*$, m. |
| θ | volumetric water fraction. |
| μ | first moment. |
| λ | correlation scale, m. |
| ρ | dry bulk density, kg m ⁻³ . |

REFERENCES

- Amoozegar-Fard, A., D. R. Nielsen, and A. W. Warrick, Soil solute concentration distributions for spatially varying pore water velocities and apparent diffusion coefficients, *Soil Sci. Soc. Am. J.*, **46**, 3-9, 1982.
- Aris, R., On the dispersion of a solute in a fluid flowing through a tube, *Proc. R. Soc. London, Ser. A*, **235**, 67-77, 1956.
- Bellin, A., Numerical generation of random fields with specified spatial correlation structure, internal report, Dep. of Civ. Eng., University of Trent, Trent, Italy, 1991.
- Bellin, A., P. Salandin, and A. Rinaldo, Simulation of dispersion in heterogeneous porous formations: statistics, first-order theories, convergence of computations, *Water Resour. Res.*, **28**, 2211-2227, 1992.
- Black, T. C., and D. L. Freyberg, Stochastic modeling of vertically averaged concentration uncertainty in a perfectly stratified aquifer, *Water Resour. Res.*, **23**, 997-1004, 1987.
- Boekhold, A. E., S. E. A. T. M. van der Zee, and F. A. M. de Haan, Prediction of cadmium accumulation in a heterogeneous soil using a scaled sorption model, Proceedings of ModelCARE 90: Calibration and Reliability in Groundwater Modelling, *IAHS Publ.*, **195**, 211-220, 1990.
- Boekhold, A. E., S. E. A. T. M. van der Zee, and F. A. M. de Haan, Spatial patterns of cadmium contents related to soil heterogeneity, *Water Air Soil Pollut.*, **57-58**, 479-488, 1991.
- Bosma, W. J. P., and S. E. A. T. M. van der Zee, Analytical approximations for nonlinear adsorbing solute transport in layered soil, *J. Contam. Hydrol.*, **10**, 99-118, 1992a.
- Bosma, W. J. P., and S. E. A. T. M. van der Zee, Analytical approximation for nonlinear adsorbing solute transport and first order degradation, *Transp. Porous Media*, in press, 1992b.
- Bresler, E., and G. Dagan, Solute dispersion in unsaturated heterogeneous soil at field scale, 2, Applications, *Soil Sci. Soc. Am. J.*, **43**, 467-472, 1979.
- Bresler, E., and G. Dagan, Convective and pore scale dispersive solute transport in unsaturated heterogeneous fields, *Water Resour. Res.*, **17**, 1685-1693, 1981.
- Bresler, E., and G. Dagan, Unsaturated flow in spatially variable fields, 3, Solute transport models and their applications to two fields, *Water Resour. Res.*, **19**, 429-435, 1983.
- Calvet, R., M. Tercé, and J. C. Arvieu, Adsorption des pesticides par les sols et leurs constituants, III, Caractéristiques généraux de l'adsorption des pesticides, *Ann. Agron.*, **31**, 239-257, 1980.
- Cameron, D. A., and A. Klute, Convective-dispersive solute transport with a combined equilibrium and kinetic adsorption model, *Water Resour. Res.*, **13**, 183-188, 1977.
- Chardon, W. J., Mobiliteit van cadmium in de bodem, Ph.D. thesis, 200 pp., Agric. Univ., Wageningen, Netherlands, 1984.
- Chrysikopoulos, C. V., P. K. Kitanidis, and P. V. Roberts, Analysis of one-dimensional solute transport through porous media with spatially variable retardation factor, *Water Resour. Res.*, **26**, 437-446, 1990.
- Coats, K. H., and B. D. Smith, Dead-end pore volume and dispersion in porous media, *Soc. Pet. Eng. J.*, **4**, 73-84, 1964.
- Cvetkovic, V. D., and A. M. Shapiro, Mass arrival of sorptive solute in heterogeneous porous media, *Water Resour. Res.*, **26**, 2057-2067, 1990.
- Dagan, G., Time-dependent macrodispersion for solute transport in anisotropic heterogeneous aquifers, *Water Resour. Res.*, **24**, 1491-1500, 1988.
- Dagan, G., *Flow and Transport in Porous Formations*, Springer-Verlag, New York, 1989.
- Dagan, G., and E. Bresler, Solute dispersion in unsaturated heterogeneous soil at field scale, 1, Theory, *Soil Sci. Soc. Am. J.*, **43**, 461-467, 1979.
- Dawson, C. N., and M. F. Wheeler, Characteristic methods in modeling nonlinear adsorption in contaminant transport, in *Computational Methods in Subsurface Hydrology*, edited by G. Gambolati, A. Rinaldo, C. A. Brebbia, W. G. Gray, and G. F. Pinder, pp. 305-314, Springer-Verlag, New York, 1990.
- de Haan, F. A. M., S. E. A. T. M. van der Zee, and W. H. van Riemsdijk, The role of soil chemistry and soil physics in protecting soil quality: Variability of sorption and transport of cadmium as an example, *Neth. J. Agric. Sci.*, **35**, 347-359, 1987.
- Destouni, G., and V. Cvetkovic, Field scale mass arrival of sorptive

Acknowledgments. This work was partly funded by Directorate for General Science, Research and Development, of the Commission of the European Communities, via the European Community Environmental Research Program STEP-CT900031. The authors gratefully acknowledge A. Bellin and A. Rinaldo for reviewing the manuscript and giving valuable suggestions.

- solute into the groundwater, *Water Resour. Res.*, 27, 1315-1325, 1991.
- Graham, W. D., and D. B. McLaughlin, A stochastic model of solute transport in groundwater: Application to the Borden, Ontario, tracer test, *Water Resour. Res.*, 27, 1345-1359, 1991.
- Jury, W. A., Simulation of solute transport using a transfer function model, *Water Resour. Res.*, 18, 363-368, 1982.
- Jury, W. A., G. Sposito, and R. E. White, A transfer function model of solute transport through soil, 1, Fundamental concepts, *Water Resour. Res.*, 22, 243-247, 1986.
- Lapidus, L., and N. R. Amundsen, Mathematics of adsorption in beds, VI, The effect of longitudinal diffusion in ion exchange and chromatographic column, *J. Phys. Chem.*, 56, 984-988, 1952.
- Mackay, D. M., W. P. Ball, and M. G. Durant, Variability of aquifer sorption properties in a field experiment on groundwater transport of organic solutes: Methods and preliminary results, *J. Contam. Hydrol.*, 1, 119-132, 1986a.
- Mackay, D. M., D. L. Freyberg, P. V. Roberts, and J. A. Cherry, A natural gradient experiment on solute transport in a sand aquifer, 1, Approach and overview of plume movement, *Water Resour. Res.*, 22, 2017-2029, 1986b.
- Rao, P. S. C., J. M. Davidson, R. E. Jessup, and H. M. Selim, Evaluation of conceptual models for describing nonequilibrium adsorption-desorption of pesticides during steady state flow in soils, *Soil Sci. Soc. Am. J.*, 43, 22-28, 1979.
- Valocchi, A. J., Spatial moment analysis of the transport of kinetically adsorbing solutes through stratified aquifers, *Water Resour. Res.*, 25, 273-279, 1989.
- van der Zee, S. E. A. T. M., Analysis of solute redistribution in a heterogeneous field, *Water Resour. Res.*, 26, 273-278, 1990a.
- van der Zee, S. E. A. T. M., Analytical traveling wave solutions for transport with nonlinear and nonequilibrium adsorption, *Water Resour. Res.*, 26, 2563-2578, 1990b. (Correction, *Water Resour. Res.*, 27, 983, 1991.)
- van der See, S. E. A. T. M., and W. H. van Riemsdijk, Transport of phosphate in a heterogeneous field, *Transp. Porous Media*, 1, 339-359, 1986.
- van der Zee, S. E. A. T. M., and W. H. van Riemsdijk, Transport of reactive solute in spatially variable soil systems, *Water Resour. Res.*, 23, 2059-2069, 1987.
- van Duijn, C. J., and P. Knabner, Travelling waves in the transport of reactive solutes through porous media: Adsorption and binary exchange, 2, *Rep. 205*, Schwerpunktprogramm der Deutsche Forschungsgemeinschaft, 45 pp., Inst. Math., Univ. Augsburg, Augsburg, Germany, 1990.
- van Genuchten, M. T., and W. J. Alves, Analytical solutions of the one-dimensional convective-dispersive transport equation, *Tech. Bull. U.S. Dep. Agric.*, 1661, 151 pp., 1982.
- van Genuchten, M. T., and P. J. Wierenga, Simulation of one-dimensional solute transfer in porous media, *Bull. 628*, 40 pp., Agric. Exp. Stn., N. M. State Univ., Las Cruces, 1974.
- van Genuchten, M. T., and P. J. Wierenga, Mass transfer studies in sorbing porous media, I, Analytical solutions, *Soil Sci. Soc. Am. J.*, 40, 473-480, 1976.
- van Genuchten, M. T., J. M. Davidson, and P. J. Wierenga, An evaluation of kinetic and equilibrium equations for the prediction of pesticide movement through porous media, *Soil Sci. Soc. Am. J.*, 38, 29-35, 1974.

W. J. P. Bosma and S. E. A. T. M. van der Zee, Department of Soil Science and Plant Nutrition, Agricultural University, P. O. Box 8005, 6700 EC Wageningen, Netherlands.

(Received November 7, 1991;
revised July 28, 1992;
accepted August 6, 1992.)